

## BENDING VIBRATIONS OF A ROTATING NON-UNIFORM BEAM WITH AN ELASTICALLY RESTRAINED ROOT

S. Y. LEE

Mechanical Engineering Department, National Cheng Kung University, Tainan,  
Taiwan 700, Republic of China

AND

Y. H. KUO

Aeronautical Research Laboratory, Taichung, Taiwan 400, Republic of China

(Received 27 February 1990, and accepted in revised form 7 March 1991)

The influence of taper ratio, elastic root restraint, setting angle and rotational speed on the bending natural frequencies of a rotating non-uniform beam is investigated using a semi-exact numerical method. One observes that the influence of taper ratio on the second and third natural frequencies of a rotating beam with constant width and linearly varied depth and a double-tapered beam is greater than that of a beam with constant depth and linearly varied width. For a beam with rotational flexibility only, the first three natural frequencies of the rotating beam are greater than those of the non-rotating beam. The second and third natural frequencies of a rotating beam with translational flexibility are greater than those of the non-rotating beam. However, the fundamental natural frequency of the rotating beam can be less than that of the non-rotating beam. In particular, when the translational rigidity of the root is relatively low and the setting angle and rotational speed of the beam are relatively high, the value of the natural frequency becomes pure imaginary and the phenomenon of divergence instability occurs. The natural frequencies are decreased when the setting angle is increased, and the influence of the setting angle on the natural frequencies becomes very significant when the phenomenon of divergence instability is about to occur.

### 1. INTRODUCTION

Rotating beams, which have importance in many practical applications, such as turbine blades, airplane propellers, and rotating space booms, have been studied by numerous investigators [1–15]. The vibrational analysis of the structures leads to a fourth order differential equation with variable coefficients. In general, except for some particular cases [1, 2], no exact closed form solution is available. Hence, many different approximate methods, such as the Rayleigh-Ritz method [3, 4], the Myklestad method [5], the finite element method [6, 7], the transfer matrix method [8], the perturbation method [9], the successive approximation method [10] and the Galerkin method [11, 12], have been used to obtain numerical results and to investigate the influence of various physical parameters on the natural frequencies of the rotating beams. However, most of these numerical methods either require a refined discretization of the domain, leading to a large system of equations and cumbersome computation, or are restricted by their rate of convergence.

In most of the previous analyses [2, 4–10], rotating beams were often modelled as cantilever beams vibrating in flexure. It has been shown analytically that the bending

frequencies of rotating cantilever beams, because of centrifugal stiffening, are higher than those of non-rotating beams [10, 13]. However, in practice, the flexibility at the root of the rotating beams is not always negligible, especially in bladed disk assemblies with complex fixtures, such as "fir tree" or "pin joint" roots. The actual beam root conditions may be regarded as elastically restrained conditions. Even though the effect of the root flexibility on the natural frequencies of non-rotating beams has been studied fully, a review of the recent literature reveals that the effect of the root flexibility on the natural frequencies of rotating beams, especially rotating non-uniform beams, has not been studied extensively [11, 12, 14, 15].

In this paper, a semi-exact numerical method, which is a generalization of the method developed by Lee and his colleagues [16, 17], is used to investigate the influence of the taper ratio, the elastic root restraint, the setting angle and the rotational speed on the bending natural frequencies of a rotating non-uniform, inextensional, straight and untwisted beam, where the Coriolis forces are neglected and the mass, centroidal and elastic axes are coincident. Several newly observed facts and conclusions are presented.

## 2. GOVERNING EQUATION AND CHARACTERISTIC EQUATION

Consider the free transverse bending vibrations of an elastic non-uniform Bernoulli-Euler beam, elastically restrained mounted with setting angle  $\theta$  on a hub with a radius  $r_0$ , rotating with constant angular velocity  $\Omega$ , as shown in Figure 1. For time harmonic vibration with angular frequency  $\omega$ , the flexural displacement  $W(X)$  satisfies the characteristic differential equation [1, 2]

$$\frac{d^2}{dX^2} \left[ E(X) I(X) \frac{d^2 W}{dX^2} \right] - \frac{d}{dX} \left[ N(X) \frac{dW}{dX} \right] - m(X)(\omega^2 + \Omega^2 \sin^2 \theta) W = 0, \quad X \in (0, l), \quad (1)$$

where  $E(X)$ ,  $I(X)$  and  $m(X)$  denote the Young's modulus, the moment of inertia and the mass per unit length of beam, respectively.  $l$  is the length of the beam and  $N(X)$  is the

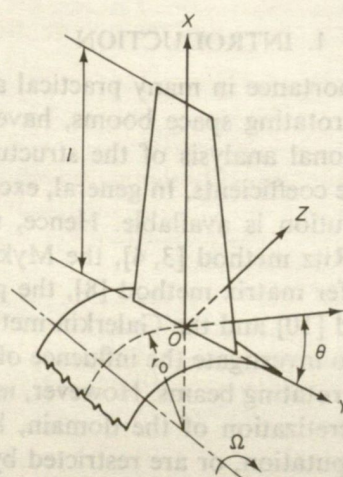


Figure 1. Beam on a rotating disk as a model of a turbomachinery blade.

centrifugal force,

$$N(X) = \Omega^2 \int_X^l m(s)(s+r_0) ds. \quad (2)$$

The associated boundary conditions are

$$\text{at } X=0, EI \frac{d^2W}{dX^2} = K_\theta \frac{dW}{dX}, \quad \frac{d}{dX} \left( EI \frac{d^2W}{dX^2} \right) - N \frac{dW}{dX} = -K_T W, \quad (3)$$

$$\text{at } X=l, \frac{d^2W}{dX^2} = 0, \quad \frac{d}{dX} \left( EI \frac{d^2W}{dX^2} \right) = 0, \quad (4)$$

where  $K_\theta$  and  $K_T$  are the rotational and translational spring stiffnesses at  $X=0$ , respectively. The spring stiffnesses are assumed to remain constant during motion.

In terms of the non-dimensional quantities

$$x = X/l, \quad V = W/l, \quad r_* = r_0/l,$$

$$\Lambda^2 = m_0 \omega^2 l^4 / E_0 I_0, \quad \alpha^2 = m_0 \Omega^2 l^4 / E_0 I_0, \quad \gamma^2 = \Lambda^2 + \alpha^2 \sin^2 \theta,$$

$$\beta_\theta = K_\theta l / E_0 I_0, \quad \beta_T = K_T l^3 / E_0 I_0, \quad G(x) = E(x)I(x)/E_0 I_0,$$

$$R(x) = \alpha^2 \left[ \frac{1}{m_0} \int_x^l m(s)(s+r_*) ds \right], \quad Q(x) = \gamma^2 \frac{m(x)}{m_0}, \quad (5)$$

where  $E_0 I_0$  and  $m_0$  are the bending rigidity and mass per unit length of the beam at the root section ( $X=0$ ) respectively, the governing characteristic differential equation can be rewritten in the non-dimensional form

$$(GV'')'' - (RV')' - QV = 0, \quad x \in (0, 1), \quad (6)$$

where the primes denote differentiations with respect to  $x$ . The associated boundary conditions become

$$\text{at } x=0, V'' - \beta_\theta V' = 0, \quad V'' + G'(0)V'' - R(0)V' + \beta_T V = 0, \quad (7)$$

$$\text{at } x=1, V'' = 0, \quad V''' = 0. \quad (8)$$

Now consider the general solution of the differential equation (6), in the form

$$V(x) = aV_1(x) + bV_2(x) + cV_3(x) + dV_4(x), \quad (9)$$

where  $a, b, c$  and  $d$  are four arbitrary constants to be determined from the specified boundary conditions. In order that the four fundamental solutions  $V_1, V_2, V_3$  and  $V_4$  are linearly independent and unique, they are chosen such that they satisfy the following normalization condition at the origin of the co-ordinate system:

$$\begin{bmatrix} V_1(0) & V_2(0) & V_3(0) & V_4(0) \\ V'_1(0) & V'_2(0) & V'_3(0) & V'_4(0) \\ V''_1(0) & V''_2(0) & V''_3(0) & V''_4(0) \\ V'''_1(0) & V'''_2(0) & V'''_3(0) & V'''_4(0) \end{bmatrix} = \begin{bmatrix} 1 & 0 & 0 & 0 \\ 0 & 1 & 0 & 0 \\ 0 & 0 & 1 & 0 \\ 0 & 0 & 0 & 1 \end{bmatrix}. \quad (10)$$

Substituting these fundamental solutions into the boundary conditions (7) and (8), and using the normalization condition (10), one obtains a set of four linearly homogeneous

equations in the four constants,  $a$ ,  $b$ ,  $c$  and  $d$ :

$$\begin{bmatrix} 0 & -\beta_\theta & 1 & 0 \\ \beta_T & -R(0) & G'(0) & 1 \\ V_1''(1) & V_2''(1) & V_3''(1) & V_4''(1) \\ V_1'''(1) & V_2'''(1) & V_3'''(1) & V_4'''(1) \end{bmatrix} \begin{bmatrix} a \\ b \\ c \\ d \end{bmatrix} = \begin{bmatrix} 0 \\ 0 \\ 0 \\ 0 \end{bmatrix}. \quad (11)$$

For non-trivial solutions, the determinant of the matrix must vanish, and this leads to the characteristic equation, in terms of the four fundamental solutions, for the natural frequencies of the rotating non-uniform beam with an elastically restrained root:

$$\begin{aligned} & [V_1''(1)V_2'''(1) - V_1'''(1)V_2''(1)] + \beta_\theta[V_1''(1)V_3'''(1) - V_1'''(1)V_3''(1)] \\ & + \beta_T[V_2''(1)V_4'''(1) - V_2'''(1)V_4''(1)] + \beta_\theta\beta_T[V_3''(1)V_4'''(1) - V_3'''(1)V_4''(1)] \\ & + (\beta_\theta G'(0) - R(0))[V_1'''(1)V_4''(1) - V_1''(1)V_4'''(1)] = 0. \end{aligned} \quad (12)$$

If the beam is cantilevered, then by setting  $\beta_\theta \rightarrow \infty$  and  $\beta_T \rightarrow \infty$ , the characteristic equation (12) becomes

$$V_3''(1)V_4'''(1) - V_3'''(1)V_4''(1) = 0. \quad (13)$$

As a result, if normalized fundamental solutions which are either exact or approximate solutions are available then, after substituting these fundamental solutions into the characteristic equation, the natural frequencies can be obtained through finding roots of the characteristic equation by the half-interval search method. After substituting the natural frequency into equation (11), one has the ratios  $b/a$ ,  $c/a$  and  $d/a$ . Consequently, the mode shapes can be obtained from equation (9).

### 3. APPROXIMATE NORMALIZED FUNDAMENTAL SOLUTIONS

For a rotating non-uniform beam, the exact closed form fundamental solutions, in general, are not available. Hence, approximate fundamental solutions are required. To find approximate fundamental solutions for general rotating non-uniform beams, consisting of beams with continuous or discontinuous bending rigidity, a simple algorithm is presented.

Upon approximating the coefficients of the governing characteristic differential equation  $G(x)$ ,  $R(x)$  and  $Q(x)$  by  $n$  piecewise constants  $G_S$ ,  $R_S$  and  $Q_S$ , respectively, the governing characteristic differential equation (6) becomes a fourth order ordinary differential equation with piecewise constant coefficients,

$$\frac{d^4 V(x)}{dx^4} - \bar{R}(x) \frac{d^2 V(x)}{dx^2} - \bar{Q}(x) V(x) = 0, \quad x \in (0, 1), \quad (14)$$

with

$$\bar{R}(x) = \begin{cases} \bar{R}_1 = R_1/G_1, & x \in (l_0 = 0, l_1) \\ \vdots & \vdots \\ \bar{R}_i = R_i/G_i, & x \in (l_{i-1}, l_i) \\ \vdots & \vdots \\ \bar{R}_n = R_n/G_n, & x \in (l_{n-1}, l_n = 1) \end{cases}, \quad (15)$$

$$\bar{Q}(x) = \begin{cases} \bar{Q}_1 = Q_1/G_1, & x \in (l_0 = 0, l_1) \\ \vdots & \vdots \\ \bar{Q}_i = Q_i/G_i, & x \in (l_{i-1}, l_i) \\ \vdots & \vdots \\ \bar{Q}_n = Q_n/G_n, & x \in (l_{n-1}, l_n = 1) \end{cases}, \quad (16)$$

where  $\bar{R}_i$  and  $\bar{Q}_i$  are constants, and  $l_i$  represent the co-ordinate positions at the ends of the respective step sections. Here  $G_i = G(x_i)$ ,  $R_i = R(x_i)$  and  $Q_i = Q(x_i)$ ; depending on the manner of approximation,  $x_i$  can be any position within the  $i$ th interval. When  $n \rightarrow \infty$ , the approximated system becomes the original system and the approximate fundamental solutions for the approximate system become the exact solutions.

By requiring the displacement, slope, bending moment and shear force to be continuous at the interface of the  $i$ th and the  $(i+1)$ th sections, the fundamental solutions in the subdomains,  $(l_i, l_{i+1})$ ,  $i \geq 1$ , can be generated from those of the neighboring subdomains,  $(l_{i-1}, l_i)$ , by the recurrence relation

$$\begin{aligned} V_{j,i+1}(x) &= \tilde{V}_{1,i+1}(x-l_i)V_{j,i}(l_i) + \tilde{V}_{2,i+1}(x-l_i)V'_{j,i}(l_i) \\ &\quad + \mu_{i+1}\{\tilde{V}_{3,i+1}(x-l_i)V''_{j,i}(l_i) + \tilde{V}_{4,i+1}(x-l_i)[V'''_{j,i}(l_i) - \bar{R}_i V'_{j,i}(l_i)]\}, \\ i &= 1, 2, \dots, n-1, \quad j = 1, 2, 3, 4, \end{aligned} \quad (17)$$

where

$$\begin{aligned} \mu_{i+1} &= G_i/G_{i+1}, \quad \tilde{V}_{1,i+1}(x-l_i) = \{1/(\lambda_{i+1}^2 + \eta_{i+1}^2)\} \\ &\quad \times [\eta_{i+1}^2 \cosh \lambda_{i+1}(x-l_i) + \lambda_{i+1}^2 \cos \eta_{i+1}(x-l_i)], \\ \tilde{V}_{2,i+1}(x-l_i) &= \{1/(\lambda_{i+1}^2 + \eta_{i+1}^2)\} \times [\lambda_{i+1} \sinh \lambda_{i+1}(x-l_i) + \eta_{i+1} \sin \eta_{i+1}(x-l_i)], \\ \tilde{V}_{3,i+1}(x-l_i) &= \{1/(\lambda_{i+1}^2 + \eta_{i+1}^2)\} \times [\cosh \lambda_{i+1}(x-l_i) - \cos \eta_{i+1}(x-l_i)], \\ \tilde{V}_{4,i+1}(x-l_i) &= \{1/(\lambda_{i+1}^2 + \eta_{i+1}^2)\} \\ &\quad \times [(1/\lambda_{i+1}) \sinh \lambda_{i+1}(x-l_i) - (1/\eta_{i+1}) \sin \eta_{i+1}(x-l_i)], \end{aligned} \quad (18)$$

$$V_{1,1}(x) = \frac{1}{\lambda_1^2 + \eta_1^2} [\eta_1^2 \cosh \lambda_1 x + \lambda_1^2 \cos \eta_1 x],$$

$$V_{2,1}(x) = \frac{1}{\lambda_1^2 + \eta_1^2} \left[ \frac{\eta_1^2}{\lambda_1} \sinh \lambda_1 x + \frac{\lambda_1^2}{\eta_1} \sin \eta_1 x \right],$$

$$V_{3,1}(x) = \frac{1}{\lambda_1^2 + \eta_1^2} [\cosh \lambda_1 x - \cos \eta_1 x],$$

$$V_{4,1}(x) = \frac{1}{\lambda_1^2 + \eta_1^2} \left[ \frac{1}{\lambda_1} \sinh \lambda_1 x - \frac{1}{\eta_1} \sin \eta_1 x \right], \quad (19)$$

and

$$\lambda_i = \sqrt{\frac{1}{2}(\bar{R}_i + \sqrt{\bar{R}_i^2 + 4\bar{Q}_i})}, \quad \eta_i = \sqrt{\frac{1}{2}(-\bar{R}_i + \sqrt{\bar{R}_i^2 + 4\bar{Q}_i})}, \quad i = 1, 2, \dots, n. \quad (20)$$

By taking the first, second and third derivatives of equations (17) and (18), without any further approximation, one can easily obtain  $V'_{j,i}(x)$ ,  $V''_{j,i}(x)$  and  $V'''_{j,i}(x)$ , respectively.

It can be observed that the approximate normalized fundamental solutions are linearly independent and satisfy the normalization condition (10) at the origin of the co-ordinate system. They can be obtained at any desired level of accuracy by approximating the coefficients of the governing differential equation by a suitable number of sections.

From the characteristic equation (12) and the recurrence formula (17), one can realize that, despite the number of sections approximated, the method mainly has to record the values of the fundamental solutions and their first three derivatives of two neighboring sections. Hence, it does not require large computer storage and CPU time.

#### 4. NUMERICAL RESULTS AND DISCUSSION

From the governing characteristic differential equation (1) and the associated boundary conditions (3) and (4), one can observe that the natural frequencies of the system are affected by the following parameters: (a) the boundary conditions; (b) the non-uniform bending rigidity  $E(X)I(X)$  and the mass  $m(X)$  per unit length of the beam; (c) the centrifugal stiffening force  $N(X)$ , which is a function of the rotational speed, the hub radius and  $m(X)$ ; (d) the softening force  $m(X)\Omega^2 \sin^2 \theta$ , which is a function of the rotational speed, the setting angle and  $m(X)$ . Since most of the physical parameters are coupled together, the influence of these physical parameters on the natural frequencies is rather complicated. Here, a numerical investigation of the influence of the non-uniform bending rigidity and mass per unit length, rotational speed, setting angle and elastic springs at the root on the natural frequencies of the beam is presented. The  $i\Lambda$  in the ordinate of Figures 5(b), 6 and 7(b) represents a pure imaginary value of frequency.

To demonstrate the convergence and efficiency of the proposed numerical method, the third and the tenth natural frequencies of a cantilever tapered beam are determined. In Figure 2, the  $g_a$  curves show the natural frequencies of the beam when the number of sections increases. Here the coefficients  $G(x)$  and  $R(x)$  in equation (6) are approximated in the manner shown in Figure 3(a), and  $Q(x)$  is approximated in the manner shown in Figure 3(b). Due to the additional value of the restoring force, the natural frequencies approach the exact values from above when the number of sections is increased. If, instead,  $G(x)$  and  $R(x)$  are approximated in the manner shown in Figure 3(b), and  $Q(x)$  is approximated in the manner shown in Figure 3(a), the natural frequencies approach the exact values from below as shown by the  $g_b$  curves in Figure 2. Here, 47·871 is the third natural frequency calculated by Hodges and Rutkowski [6] and 652·035 is the tenth natural frequency from convergence. Since the  $g_a$  and  $g_b$  curves converge from opposite directions, a more accurate result can be obtained by approximating the functions  $G(x)$ ,  $R(x)$  and  $Q(x)$  in the manner shown in Figure 3(c). The  $g_c$  curves in Figure 2 are the natural frequencies determined by this improved approximation. It can be observed that the rate of convergence has improved significantly. Even when the number of sections is only ten, the errors are less than 0·25% for the third natural frequency and 0·7% for the tenth natural frequency. In the following numerical analysis, the coefficients of the governing equation are approximated in the manner shown in Figure 3(c) and the number of sections approximated is chosen as twenty.

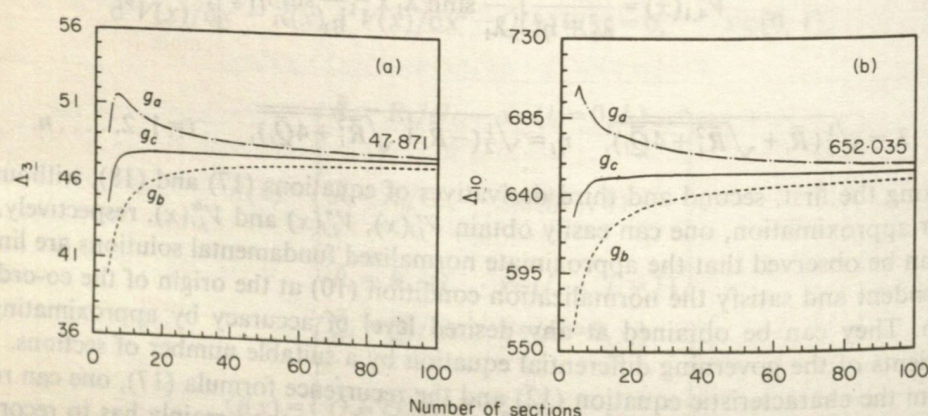


Figure 2. Convergence check of the natural frequencies of a rotating cantilever beam;  $E(X)I(X) = E_0 I_0 (1 - 0.5X/l)^3$ ,  $m(X) = m_0 (1 - 0.5X/l)$ ,  $\alpha = 2$ ,  $\theta = 0^\circ$  and  $r_* = 0$ . (a) The third natural frequency; (b) the tenth natural frequency.

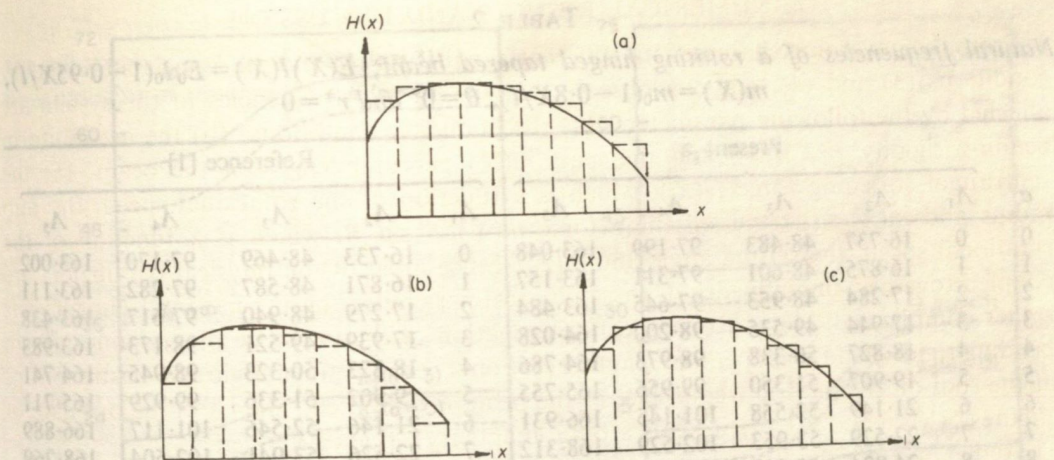


Figure 3. Approximation of function  $H(x)$ , where  $H(x)$  represents  $G(x)$  or  $R(x)$  or  $Q(x)$ .

In Tables 1 and 2 it is shown that the present results for the first three bending natural frequency parameters  $\Lambda_i$  of a rotating cantilever tapered beam and the first five bending natural frequency parameters of a rotating hinged tapered beam agree very well with the data given in reference [6] and reference [1], respectively.

The influence of the taper ratio ( $\varepsilon$ ) on the first three natural frequencies of three different cantilever beams is shown in Figure 4. It can be observed that the influence of the taper ratio on the second and third natural frequencies of a beam with constant width and linearly varied depth and a double-tapered beam is greater than that on the fundamental natural frequencies of the beams. Among the three tapered beams, the influence of the taper ratio on the second and third natural frequencies of the beam with constant depth and linearly varied width is less significant than that of the other two beams.

The influence of the root flexibility, the setting angle and the rotational speed on the first three natural frequencies of the rotating and non-rotating beams is illustrated in Figures 5-7. It is shown in Figure 5(a) that, for a beam with rotational flexibility only,

TABLE 1

Natural frequencies of a rotating cantilever tapered beam;  $E(X)I(X) = E_0 I_0(1 - 0.5X/l)^3$ ,  
 $m(X) = m_0(1 - 0.5X/l)$ ,  $\theta = 0^\circ$  and  $r^* = 0$

$\alpha$	Present			Reference [6]		
	$\Lambda_1$	$\Lambda_2$	$\Lambda_3$	$\Lambda_1$	$\Lambda_2$	$\Lambda_3$
0	3.8242	18.3198	47.2711	3.8238	18.3173	47.2648
1	3.9871	18.4763	47.4232	3.9866	18.4740	47.4173
2	4.4368	18.9373	47.8736	4.4368	18.9366	47.8716
3	5.0927	19.6840	48.6203	5.0927	19.6839	48.6190
4	5.8786	20.6847	49.6461	5.8788	20.6852	49.6456
5	6.7432	21.9040	50.9331	6.7345	21.9053	50.9338
6	7.6549	23.3071	52.4613	7.6551	23.3093	52.4633
7	8.5953	24.8618	54.2089	8.5956	24.8647	54.2124
8	9.5537	26.5398	56.1542	9.5540	26.5436	56.1595
9	10.5236	28.3180	58.2762	10.5239	28.3227	58.2833
10	11.5012	30.1770	60.5548	11.5015	30.1827	60.5639
11	12.4841	32.1018	62.9714	12.4845	32.1085	62.9829
12	13.4707	34.0799	65.5100	13.4711	34.0877	65.5237

TABLE 2

Natural frequencies of a rotating hinged tapered beam;  $E(X)I(X)=E_0I_0(1-0.95X/l)$ ,  $m(X)=m_0(1-0.8X/l)$ ,  $\theta=0^\circ$  and  $r^*=0$

$\alpha$	Present					Reference [1]				
	$\Lambda_1$	$\Lambda_2$	$\Lambda_3$	$\Lambda_4$	$\Lambda_5$	$\Lambda_1$	$\Lambda_2$	$\Lambda_3$	$\Lambda_4$	$\Lambda_5$
0	0	16.737	48.483	97.199	163.048	0	16.733	48.469	97.170	163.002
1	1	16.875	48.601	97.311	163.157	1	16.871	48.587	97.282	163.111
2	2	17.284	48.953	97.645	163.484	2	17.279	48.940	97.617	163.438
3	3	17.944	49.535	98.200	164.028	3	17.939	49.521	98.173	163.983
4	4	18.827	50.338	98.973	164.786	4	18.823	50.323	98.945	164.741
5	5	19.907	51.350	99.956	165.755	5	19.902	51.336	99.929	165.711
6	6	21.149	52.558	101.145	166.931	6	21.146	52.546	101.117	166.889
7	7	22.529	53.953	102.529	168.312	7	22.526	53.941	102.504	168.269
8	8	24.024	55.517	104.105	169.890	8	24.020	55.504	104.079	169.847
9	9	25.610	57.235	105.859	171.658	9	25.606	57.223	105.835	171.618
10	10	27.274	59.094	107.785	173.611	10	27.269	59.083	107.762	173.573
11	11	28.999	61.082	109.871	175.745	11	28.996	61.070	109.850	175.708
12	12	30.780	63.182	112.110	178.051	12	30.775	63.172	112.090	178.105

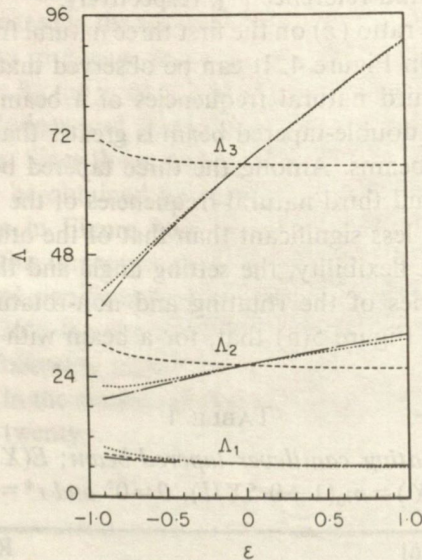


Figure 4. Influence of taper ratio on the natural frequencies of a rotating cantilever beam;  $\alpha=3$ ,  $\theta=45^\circ$  and  $r^*=2$ . ---,  $E(X)I(X)=E_0I_0(1+\varepsilon X/l)$  and  $m(X)=m_0(1+\varepsilon X/l)$ ; — · —,  $E(X)I(X)=E_0I_0(1+\varepsilon X/l)^3$  and  $m(X)=m_0(1+\varepsilon X/l)$ ; · · · · ·,  $E(X)I(X)=E_0I_0(1+\varepsilon X/l)^4$  and  $m(X)=m_0(1+\varepsilon X/l)^2$ .

the first three natural frequencies of the rotating beam are greater than those of the non-rotating beam. From Figures 5(b) and 6, it can be observed that the second and third natural frequencies of a rotating beam with translational flexibility are greater than those of the non-rotating beam. However, when  $\beta_T$  is less than  $b_0$ , the fundamental natural frequency of the rotating beam can be less than that of the non-rotating beam. In particular, when the translational rigidity of the root is relatively low, say  $\beta_T$  is less than  $a_0$ , and the setting angle and rotational speed of the beam are relatively high, the value of the fundamental natural frequency becomes pure imaginary and the phenomenon of divergence instability occurs. This physical phenomenon is mainly due to the coupling effect of the

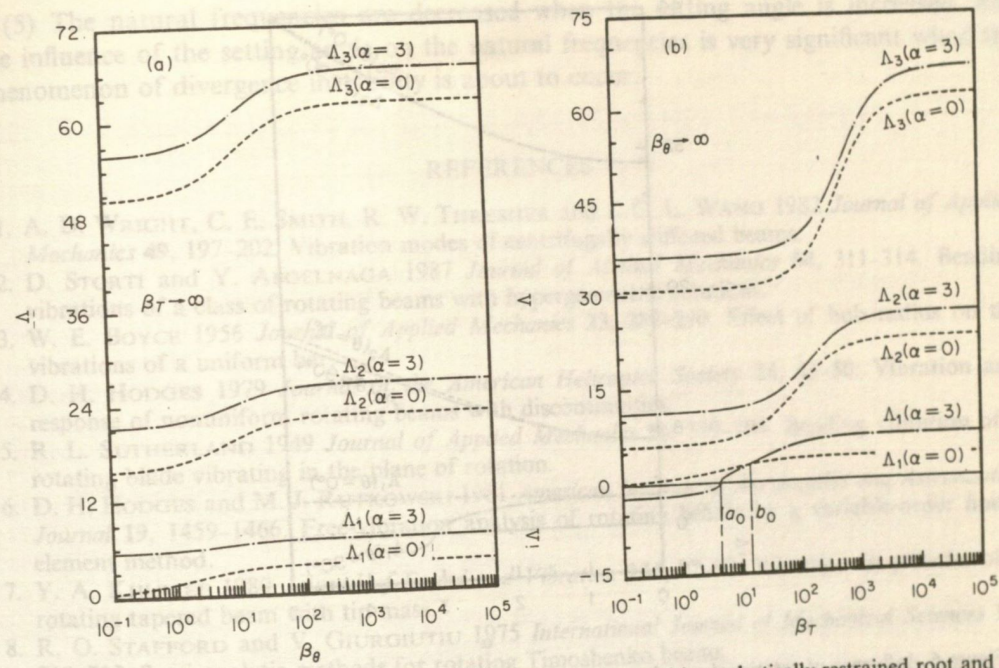


Figure 5. Natural frequencies of rotating and non-rotating beams with an elastically restrained root and (a) with rotational flexibility only, (b) with translational flexibility only.  $E(X)I(X) = E_0 I_0(1 - 0.2X/l)$ ,  $m(X) = m_0(1 - 0.2X/l)$ ,  $\theta = 45^\circ$  and  $r_* = 2$ .

boundary conditions and the softening force, which becomes greater than the centrifugal stiffening force. One can consider this new observation as the generalization of the conclusion given by Schilhansl [10] and Pnueli [13]. They had shown analytically that the fundamental natural frequency of a rotating cantilever uniform beam is greater than that of a non-rotating beam. Finally, from Figures 6 and 7, it can also be observed that the natural frequencies are decreased when the setting angle is increased, and the influence of the setting angle on the natural frequencies is very significant when the phenomenon of divergence instability is about to occur.

## 5. CONCLUSIONS

The influence of the taper ratio, the elastic root restraint, the setting angle and the rotational speed on the natural frequencies of a rotating non-uniform beam has been investigated numerically using a semi-exact numerical method which can easily be extended to the analysis of free vibrations of general non-uniform Bernoulli-Euler beams, such as a generally elastically end restrained non-uniform beam resting on non-uniform two-parameter elastic foundation. Due to the coupling effect of (a) the boundary conditions, (b) the non-uniform bending rigidity and the mass per unit length of the beam, (c) the centrifugal stiffening force and (d) the softening force, the following behavioral trends have been found.

- (1) The influence of the taper ratio on the second and third natural frequencies of a beam with constant width and linearly varied depth and a double-tapered beam is greater than that on the fundamental natural frequencies of the beams.
- (2) Among the three tapered beams, the influence of the taper ratio on the second and third natural frequencies of the beam with constant depth and linearly varied width is less significant than that of the other two beams.

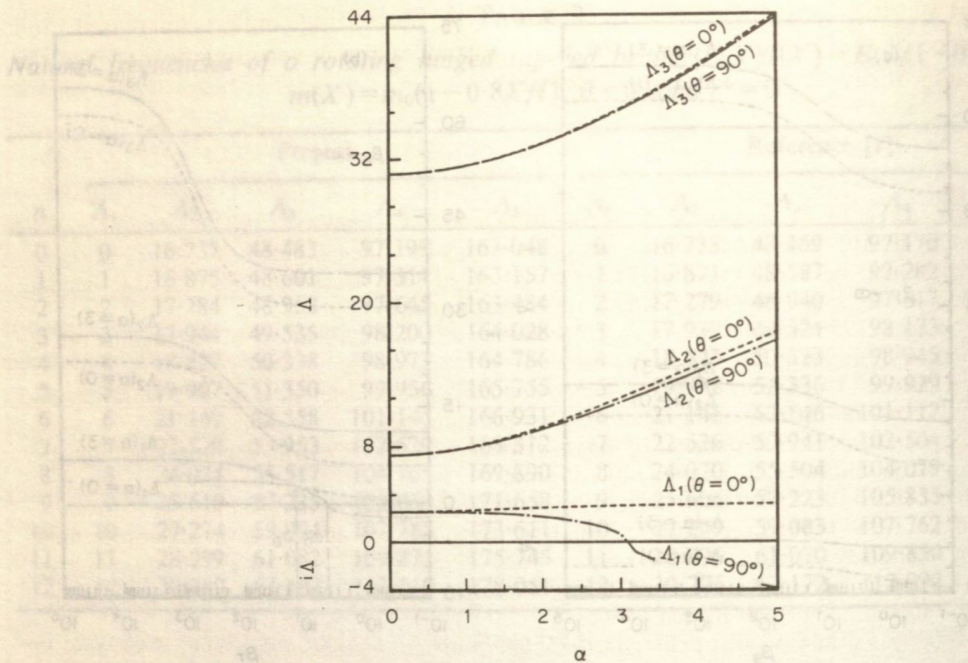


Figure 6. Influence of rotational speed on the natural frequencies of a rotating non-uniform beam with an elastically restrained root for different values of setting angle.  $E(X)I(X) = E_0 I_0(1 - 0.2X/l)$ ,  $m(X) = m_0(1 - 0.2X/l)$ ,  $\beta_\theta = 100$ ,  $\beta_T = 10$  and  $r_* = 2$ .

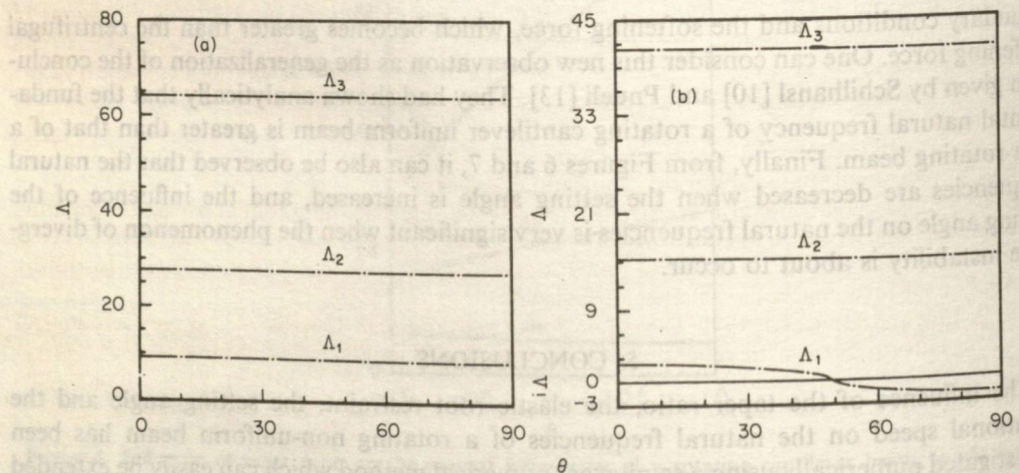


Figure 7. Influence of setting angle on the natural frequencies of a rotating beam with an elastically restrained root and (a) with rotational flexibility only ( $\beta_\theta = 5$ ,  $\beta_T \rightarrow \infty$ ), (b) with translational flexibility only ( $\beta_\theta \rightarrow \infty$ ,  $\beta_T = 5$ ).  $E(X)I(X) = E_0 I_0(1 - 0.2X/l)$ ,  $m(X) = m_0(1 - 0.2X/l)$ ,  $\alpha = 3$  and  $r_* = 5$ .

(3) For a beam with rotational flexibility only, the natural frequencies of the rotating beam are greater than those of the non-rotating beam.

(4) The second and third natural frequencies of a rotating beam with translational flexibility are greater than those of the non-rotating beam. However, the fundamental natural frequency of the rotating beam can be less than that of the non-rotating beam. In particular, when the translational rigidity of the root is relatively low and the setting angle and rotational speed of the beam are relatively high, the value of the natural frequency becomes pure imaginary and the phenomenon of divergence instability occurs.

(5) The natural frequencies are decreased when the setting angle is increased, and the influence of the setting angle on the natural frequencies is very significant when the phenomenon of divergence instability is about to occur.

## REFERENCES

1. A. D. WRIGHT, C. E. SMITH, R. W. THRESHER and J. C. L. WANG 1982 *Journal of Applied Mechanics* **49**, 197-202. Vibration modes of centrifugally stiffened beams.
2. D. STORTI and Y. ABOELNAGA 1987 *Journal of Applied Mechanics* **54**, 311-314. Bending vibrations of a class of rotating beams with hypergeometric solutions.
3. W. E. BOYCE 1956 *Journal of Applied Mechanics* **23**, 287-290. Effect of hub radius on the vibrations of a uniform bar.
4. D. H. HODGES 1979 *Journal of the American Helicopter Society* **24**, 43-50. Vibration and response of nonuniform rotating beams with discontinuities.
5. R. L. SUTHERLAND 1949 *Journal of Applied Mechanics* **16**, 389-394. Bending vibration of a rotating blade vibrating in the plane of rotation.
6. D. H. HODGES and M. J. RUTKOWSKI 1981 *American Institute of Aeronautics and Astronautics Journal* **19**, 1459-1466. Free-vibration analysis of rotating beams by a variable-order finite-element method.
7. Y. A. KHULIEF 1989 *Journal of Sound and Vibration* **134**, 87-97. Vibration frequencies of a rotating tapered beam with tip mass.
8. R. O. STAFFORD and V. GIURGIUTIU 1975 *International Journal of Mechanical Sciences* **17**, 719-727. Semi-analytic methods for rotating Timoshenko beams.
9. H. LO, J. E. GOLDBERG and J. L. BOGDANOFF 1960 *Journal of Applied Mechanics* **27**, 548-550. Effect of small hub-radius change on bending frequencies of a rotating beam.
10. M. J. SCHILHANSI 1958 *Journal of Applied Mechanics* **25**, 28-30. Bending frequency of a rotating cantilever beam.
11. W. H. LIU and F. H. YEH 1987 *Journal of Sound and Vibration* **119**, 379-384. Vibrations of non-uniform rotating beams.
12. F. H. YEH and W. H. LIU 1989 *Journal of the Chinese Society of Mechanical Engineers* **10**, 393-400. Transverse vibrations of non-uniform rotating beams with rotational and translational restraints.
13. D. PNUEL 1972 *Journal of Applied Mechanics* **39**, 602-604. Natural bending frequency comparable to rotational frequency in rotating cantilever beam.
14. A. W. LEISSA 1981 *Applied Mechanics Reviews* **34**, 629-635. Vibrational aspects of rotating turbomachinery blades.
15. V. RAMAMURTI and P. BALASUBRAMANIAN 1984 *The Shock and Vibration Digest* **16**, 13-28. Analysis of turbomachinery blades—a review.
16. S. Y. LEE and H. Y. KE 1990 *Journal of Sound and Vibration* **136**, 425-437. Free vibrations of a non-uniform beam with general elastically restrained boundary conditions.
17. S. Y. LEE, H. Y. KE and Y. H. KUO 1990 *Computers and Structures* **36**, 91-97. Exact static deflection of a non-uniform Bernoulli-Euler beam with general elastic end restraints.

stillness layers in order to introduce layerwise boundary conditions. It has been investigated that increase the thickness deformation of the damping layers [6, 7]. Additional design approaches can be found in the use of anisotropic and lamination techniques.

When anisotropic stiffness materials are incorporated into damped composite components, a coupling between normal and shear effects (stress coupling) is created. Stress coupling produces components of strain in the damping layers that do not occur in isotropic designs while retaining and adding to those components that already do occur. Conceivably, this increased amount of the damping material would lead to higher energy dissipation and improved structural performance.

Lamination can be used to favorably change the stiffness of a damped beam. One can consider a damped composite plate with two outer stiffness layers that are replaced by one. If the stiffness of the stiffening layers is greater than the outer stiffness layers, the beam will have more bending stiffness but directly reduce the stiffness of the damping surfaces.